JCI insight

Free light chains injure proximal tubule cells through the STAT1/HMGB1/TLR axis

Rohit Upadhyay, … , Paul W. Sanders, Vecihi Batuman

JCI Insight. 2020;5(14):e137191. https://doi.org/10.1172/jci.insight.137191.

Research Article | Cell biology | Nephrology

Graphical abstract

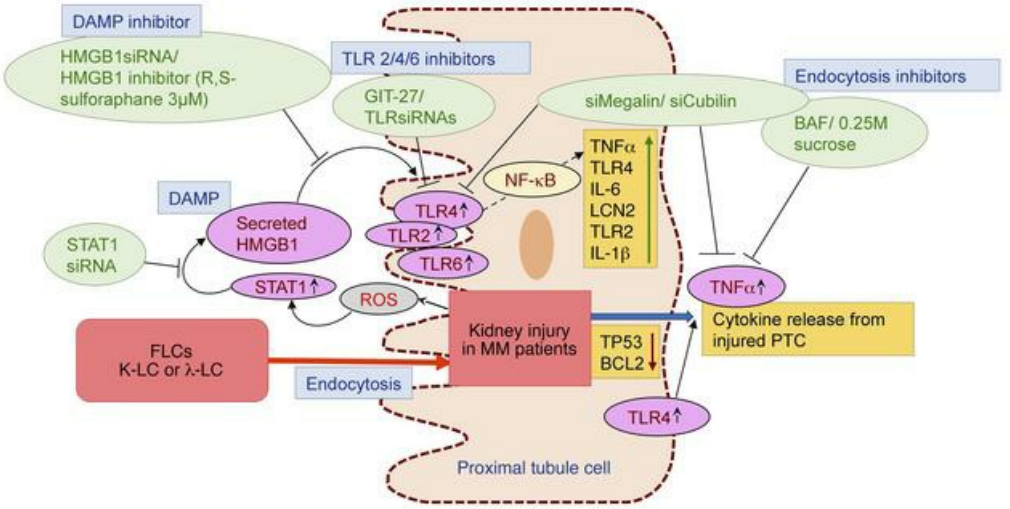

Find the latest version:

https://jci.me/137191/pdf

JCI insight

RESEARCH ARTICLE

Free light chains injure proximal tubule cells through the STAT1/HMGB1/TLR axis

Rohit Upadhyay,[1] Wei-Zhong Ying,[2] Zannatul Nasrin,[1] Hana Safah,[1] Edgar A. Jaimes,[3] Wenguang Feng,[2] Paul W. Sanders,[2,4] and Vecihi Batuman[1,5]

[1]John W. Deming Department of Medicine, Tulane University School of Medicine, New Orleans, Louisiana, USA. [2]University of Alabama at Birmingham, Birmingham, Alabama, USA. [3]Department of Medicine, Renal Service, Memorial Sloan Kettering Cancer Center, New York, New York, USA. [4]Department of Veterans Affairs Medical Center, Birmingham, Alabama, USA. [5]Department of Veterans Affairs Southeast Louisiana Veterans Health Care System, New Orleans, Louisiana, USA.

Free light chains (FLCs) induce inflammatory pathways in proximal tubule cells (PTCs). The role of TLRs in these responses is unknown. Here we present findings on the role of TLRs in FLC-induced PTC injury. We exposed human kidney PTC cultures to κ and λ FLCs and used cell supernatants and pellets for ELISA and gene expression studies. We also analyzed tissues from *Stat1*$^{-/-}$ and littermate control mice treated with daily i.p. injections of a κ FLC for 10 days. FLCs increased the expression of TLR2, TLR4, and TLR6 via HMGB1, a damage-associated molecular pattern. Countering TLR2, TLR4, and TLR6 through GIT-27 or specific TLR siRNAs reduced downstream cytokine responses. Blocking HMGB1 through siRNA or pharmacologic inhibition, or via STAT1 inhibition, reduced FLC-induced TLR2, TLR4, and TLR6 expression. Blocking endocytosis of FLCs through silencing of megalin/cubilin, with bafilomycin A1 or hypertonic sucrose, attenuated FLC-induced cytokine responses in PTCs. IHC showed decreased TLR4 and TLR6 expression in kidney sections from *Stat1*$^{-/-}$ mice compared with their littermate controls. PTCs exposed to FLCs released HMGB1, which induced expression of TLR2, TLR4, and TLR6 and downstream inflammation. Blocking FLCs' endocytosis, *Stat1* knockdown, HMGB1 inhibition, and TLR knockdown each rescued PTCs from FLC-induced injury.

Introduction

Multiple myeloma (MM) is a cancer of mature B cells or plasma cells. In healthy state, plasma cells produce a slight excess of immunoglobulin free light chains (FLCs), both κ and λ, that are efficiently endocytosed and catabolized by the kidney proximal tubule cells (PTCs), and only minute amounts of FLC proteins normally appear in the urine (1). In MM, FLCs are produced in excessive quantities and overwhelm the endocytic capacity of PTCs (2). Overloading endocytic pathways elicits cell stress responses that result in activation of inflammatory pathways and cell injury, leading to a worse prognosis in patients with MM (2–4). Nephrotoxic effects of FLCs include a cascade of inflammatory effects, such as generation of reactive oxygen species and activation of MAPK and NF-κB, followed by transcription and secretion of inflammatory and profibrotic cytokines, apoptosis, and epithelial–mesenchymal transition of PTCs (5–11).

In the initial stages, the kidney effects may appear as subtle proximal tubule function alterations including Fanconi syndrome (7–9). These changes often progress to more severe tubulointerstitial kidney disease leading to either acute kidney injury or chronic tubulointerstitial disease with or without cast nephropathy (1, 7, 8, 12–14). In many cases, the progression of kidney disease is indolent and often recognized late with the consequence of delayed therapy further compromising prognosis.

Although a clearer picture of the inflammatory events surrounding FLC nephrotoxicity has emerged from the recent studies, there are still unanswered questions. For example, an overview of the inflammatory phenomena noted in PTCs exposed to FLCs and in animal models (6, 9) raises the possibility that innate immunity may play a role, but this has not been investigated in the setting of FLC cytotoxicity. In this current work, we present our findings on the role of TLRs, tools of innate immunity, in the inflammatory effects of myeloma FLCs on human PTCs.

Authorship note: PWS and VB contributed equally to this work.

Conflict of interest: EAJ is the chief medical officer and a shareholder of Goldilocks Therapeutics Inc.

Submitted: February 27, 2020
Accepted: June 10, 2020
Published: July 23, 2020.

Reference information: *JCI Insight*. 2020;5(14):e137191. https://doi.org/10.1172/jci.insight.137191.

Results

FLCs caused injury to PTCs and decreased proliferation rate in a dose-dependent manner. Expression of kidney injury marker lipocalin 2 (LCN2), also known as neutrophil gelatinase–associated lipocalin, was increased in PTCs (HK2 cells) exposed to FLCs (T-κ1 or T-λ1) for 24 hours but not in control cells (Figure 1A). Cell proliferation of PTCs decreased significantly upon exposure to high concentrations (200–400 μM) of FLCs (6): T-κ (3) and T-λ (3) for 24 hours (Supplemental Figure 1; supplemental material available online with this article; https://doi.org/10.1172/jci.insight.137191DS1). The 25-μM concentration of FLCs selected for the present study corresponds to the levels expected in patients with MM with modest FLC proteinuria (4).

LCN2 gene expression in RPTECs was upregulated when incubated with T-κ1 and T-λ1 FLCs (25 μM each for 24 hours; $n = 5$), in comparison with untreated (no LC) or BSA-treated (160 μM) cells (Figure 1B).

FLCs induced significant upregulation of kidney injury biomarkers. Screening of candidate genes (*TLR2*, *TLR3*, *TLR4*, *TLR6*, *TLR9*, *HMGβ1*, *MYD88*, *TICAM1*, *IL6*, *IL18*, *IL1β*, *IL2*, *TNFα*, *TGFβ*, *BCL2*, *TP53*, *HAVCR1*, *ABCβ1*, and *LCN2*) was performed by quantitative PCR (qPCR) to associate their expressions with injury in PTCs exposed with 6 different FLCs ($n = 5$ in each group) for 24 hours. A heatmap of gene expressions was constructed with hierarchical clustering of the data (Figure 2). We found that *TNFα*, *TLR4*, *MYD88*, *IL6*, *LCN2*, *CUBN*, *TLR2*, and *IL-1β* were upregulated in PTCs exposed to 6 different FLCs, whereas *TP53* and *BCL2* were downregulated.

TNF-α appeared prominently among the top candidate gene markers in PTCs exposed to FLCs. To validate this observation, we checked TNF-α protein levels in PTCs after exposure to varying concentrations (25–400 μM) of T-κ1 and T-λ1 FLCs for 24 hours or 48 hours. TNF-α levels increased in PTCs in a dose- and time-dependent manner after exposure to either FLC isotype ($P < 0.05$; Figure 3, A and B). We used this assay as an indicator of FLCs toxicity in PTCs throughout this study.

FLCs upregulated the expression of TLR2, TLR4, and TLR6 and their downstream adaptor protein molecules MYD88 and TRIF. After exposure to 6 different FLCs (3 T-κ and 3 T-λ), the mRNA and protein levels of TLR2, TLR4, and TLR6 were significantly upregulated in PTCs ($P < 0.05$; Figure 4 A–D, G–I). Specifically, TLR4 was significantly upregulated by 6 different FLCs. Both MyD88- and TRIF-dependent pathways were activated because mRNA expression of both adaptor proteins were significantly upregulated (Figure 4, E and F); however, MYD88 was more significantly upregulated with most of the FLCs used in these studies (5 of the 6 FLCs).

PTCs released HMGB1 into the medium when exposed to the FLCs. Activation of TLR is mediated by unique ligands, such as pathogen-associated molecular patterns or damage-associated molecular patterns (DAMPs). HMGB1 is one of the key DAMPs that is known to activate TLR4 signaling. Therefore, we assayed HMGB1 levels by ELISA in PTCs exposed to 6 different FLCs for 24 hours. Remarkably, 6 different FLCs (3 A-κ and 3 A-λ FLCs) induced significant HMGB1 release into the medium from PTCs, in comparison with cells treated with vehicle or BSA ($n = 8$; $P < 0.05$; Figure 5A). This finding suggested that PTCs injured by exposure to FLCs release HMGB1 to activate TLRs on the PTCs.

Lu et al. showed that the JAK/STAT1 pathway participates integrally in the release of HMGB1 by promoting the hyperacetylation of multiple amino acid residues that include those within the 2 nuclear localization sites on HMGB1 (15). This posttranslational modification permits the movement of HMGB1 out of the nucleus and subsequent release into the extracellular space. Because this pathway is activated by FLCs in the proximal tubule, we hypothesized that the STAT1 pathway mediated the FLC-induced release of HMGB1. Consistent with prior results (5), the siRNA that targeted STAT1 effectively reduced STAT1 protein (Figure 5B). The reduction in STAT1 decreased the FLC-mediated HMGB1 release (Figure 5C). These data supported the role of the STAT1 pathway in this process.

FLCs induced TLR expression in vivo. Analysis of changes in mRNA expression in kidney cortex of $Stat1^{+/+}$ mice treated with FLCs for 10 days showed increased expression of TLR2, TLR4, and TLR6 compared with control mice. These increases were mitigated in $Stat1^{-/-}$ mice, although the changes in TLR4 did not differ between the $Stat1^{+/+}$ and $Stat1^{-/-}$ groups. We then performed IHC studies and attempted to stain for TLR2, TLR4, and TLR6 in kidney sections from these same $Stat1^{+/+}$ and $Stat1^{-/-}$ mice treated with FLCs (5). Whereas staining for TLR2 was unsuccessful, staining for TLR4 and TLR6 was strongly (score = 3+) or moderately strongly (score = 2+) positive in the $Stat1^{+/+}$ mice, predominantly in the proximal tubules, but was negative (score = 0) or only trace positive (score = 1+) in $Stat1^{-/-}$ mice kidneys (Figure 5, D and E). This experiment confirms that TLR activation is involved in FLC-mediated

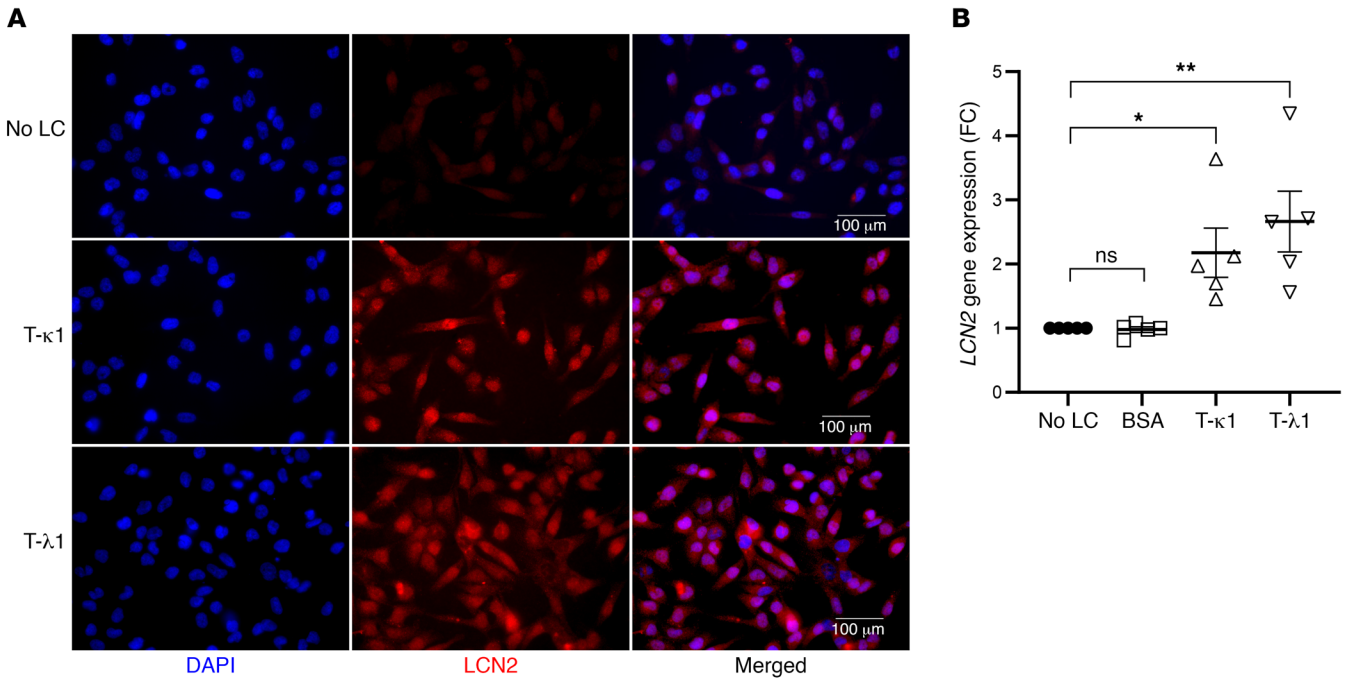

Figure 1. Free light chain exposure upregulates expression of kidney injury marker lipocalin 2 in PTCs. (**A**) T-κ1 and T-λ1 free light chains (FLC) exposure (25 μM each for 24 hours) to human PTCs (HK2) caused cellular injury, evident by the increased expression of known kidney injury marker LCN2 (DAPI, blue; LCN2, red) compared with untreated (no LC) cells. (**B**) *LCN2* gene expression significantly increased in RPTECs exposed to T-κ1 and T-λ1 FLCs (25 μM each for 24 hours; $n = 5$) compared with untreated (no LC) or BSA-treated (160 μM) cells. $^*P < 0.05$, $^{**}P < 0.01$ (1-way ANOVA followed by Tukey's multiple comparisons test). FLCs, free light chains; PTCs, proximal tubule cells; LCN2, lipocalin 2.

inflammation in the kidney and that STAT1 plays a pivotal role in the activation of inflammatory pathways in the FLC-exposed kidney.

FLCs activated TLRs through HMGB1. To validate our hypothesis that induced HMGB1 release activates TLRs, we modulated HMGB1 expression in PTCs either with introduction of extracellular HMGB1 (100ng/mL) for overexpression or with HMGB1 siRNA for inhibition of HMGB1 expression in the presence or absence of FLCs.

HMGB1 ELISA results confirmed that extracellular HMGB1 (100 ng/mL) was detectable after treatment with a T-κ and a T-λ FLC (similar to other FLCs used in Figure 5A), whereas HMGB1 siRNA inhibited HMGB1 release into the media of FLC-exposed PTCs (Figure 6A). Furthermore, we assessed the expression of TLR2, TLR4, and TLR6 in PTCs with or without FLC treatment and while modulating medium HMGB1 concentration. The addition of HMGB1 increased expression of TLR2 (2.56-fold change; $P = 0.0012$), TLR4 (1.88-fold change; $P = 0.03$), and TLR6 (1.60-fold change; $P = 0.08$) proteins. Further, HMGB1 knockdown (by siRNA or by R,S Sulforaphane) inhibited the expected increase in TLR2, TLR4, and TLR6 that occurred with FLC treatment, which suggests HMGB1 as a regulator of TLR2, TLR4, and TLR6 activation in PTCs (Figure 6, B–F).

Inhibition of TLR expression reduced FLC-induced TNF-α release. To evaluate whether the FLC-induced release of TNF-α by PTCs was mediated by TLR signaling, we treated PTCs with TLR2, TLR4, and TLR6 signaling inhibitor GIT27. Addition of the inhibitor prevented secretion of TNF-α (Figure 7, A–C), indicating that TLR activation is involved in FLC-induced cytokine release. Through dose-response analysis, we found that GIT27 at 150 μM prevented the secretion of TNF-α from the RPTECs (Figure 7D). Additionally, we used pooled sets of siRNAs to knock down *TLR2, TLR4*, and *TLR6* genes individually and in combination. We found that *TLR2/4/6*-siRNAs also reduced FLC-induced TNF-α expression in PTCs, again pointing to the role of TLR activation in production of TNF-α (Figure 7E).

Blocking endocytosis of FLCs inhibited TNF-α release and expression of TLR4 and TNF-α. We used hypertonic sucrose solution (0.25 M), which inhibits receptor-mediated endocytosis by interfering with clathrin-coated pit formation and bafilomycin A1 (1 μM), a V-ATPase inhibitor, to block endocytosis of FLCs into PTCs (12). Both of these maneuvers to inhibit endocytosis had a protective effect on PTCs exposed to FLCs

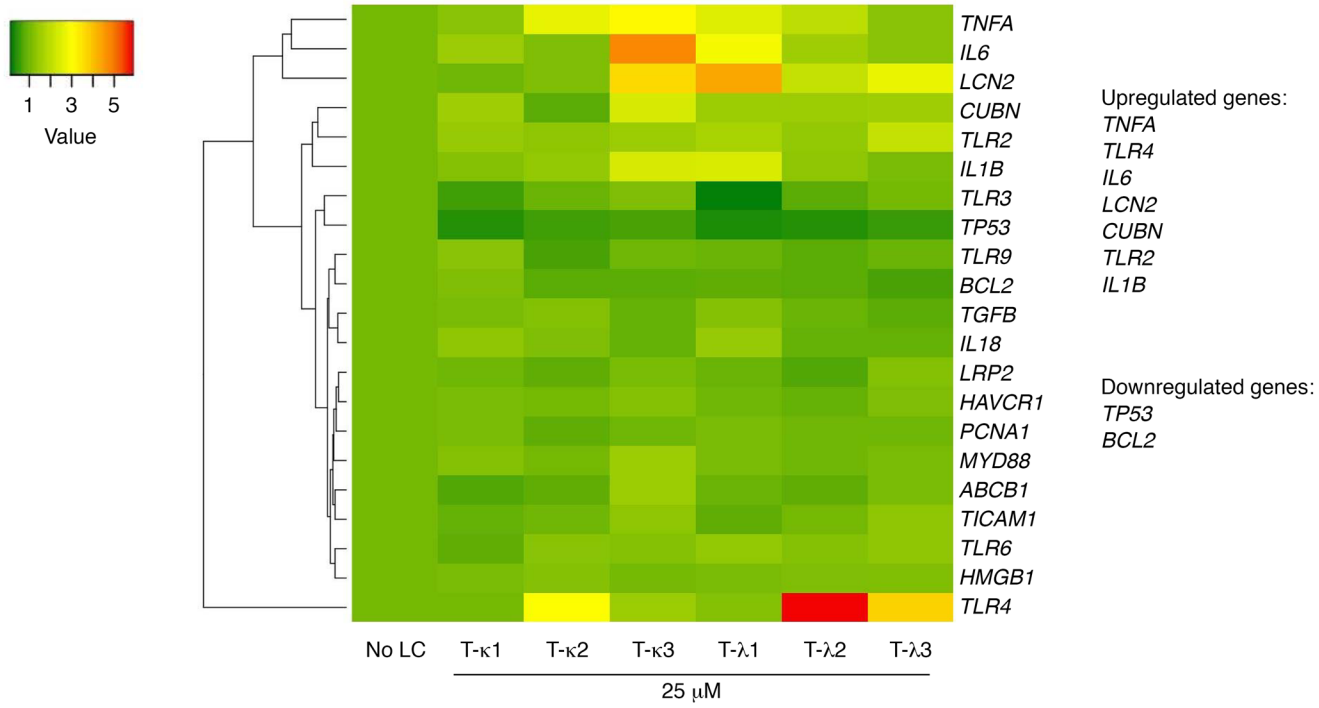

Figure 2. Heatmap of candidate gene expressions with hierarchical clustering in PTCs (RPTECs) exposed to 6 different FLCs (T-κ1, T-κ2, T-κ3, T-λ1, T-λ2, T-λ3) for 24 hours. PTCs, proximal tubule cells; FLCs, free light chains. $n = 5$.

because they both significantly decreased TNF-α release from PTCs in response to FLC exposure ($P < 0.05$, Figure 8A). Furthermore, we silenced megalin and cubilin genes using specific pooled siRNAs as another maneuver to inhibit endocytosis (4) and again noted a marked decrease in FLC-induced expressions of *TNF*α and *TLR4* genes (Figure 8, B and C).

Discussion

Up to 50% of newly diagnosed patients with MM have kidney involvement (16), which can lead to a rapid decline in organ function and organ failure (17–19) and is associated with worse prognosis in MM (20). It has been estimated that there will be 32,270 new cases of myeloma and an estimated 12,830 people may die (2.1% of all cancer deaths) of this disease in year 2020 in the United States (survival percentage in 5 years: 2010–2016, 53.9%) (21). Early diagnosis and intervention remain keys for preventing irreversible renal injury in patients with MM.

In the early stages of MM, FLC nephrotoxicity may present with proximal tubule functional abnormalities. Overproduction of monoclonal FLCs is a major factor in the pathophysiology of myeloma kidney, although a direct correlation between quantity and nephrotoxicity does not exist, indicating variable toxicity among FLC species. Our previous work demonstrated that inflammatory pathways triggered by the endocytosis of FLCs in the PTCs play a significant role in the pathophysiology of FLC-associated kidney injury (22). Studies based on in vitro exposure of kidney cells to FLCs from patients with myeloma provided considerable insight into the pathophysiology of kidney disease in MM (2–4, 10, 11, 23–25). Li et al. (4) demonstrated that FLC endocytosis is predominantly mediated by the megalin/cubilin tandem endocytic receptor, and blocking light chain endocytosis helps in preventing its nephrotoxic effects on human kidney PTCs. We also have published studies that showed endocytosis of FLC in RPTECs leads to activation of NF-κB and inflammatory pathways, along with epithelial–mesenchymal transition (4, 9, 13, 26). Although inflammatory pathways responsible for these lesions have been identified, the precise mechanisms initiating these responses are still not clear. Specifically, the role of innate immunity mediated by TLRs has not been explored. TLRs are a family of evolutionarily conserved transmembrane pattern/damage recognition receptors that can generate a cascade of signaling events that lead to the production of myriad cytokines and effector molecules (27).

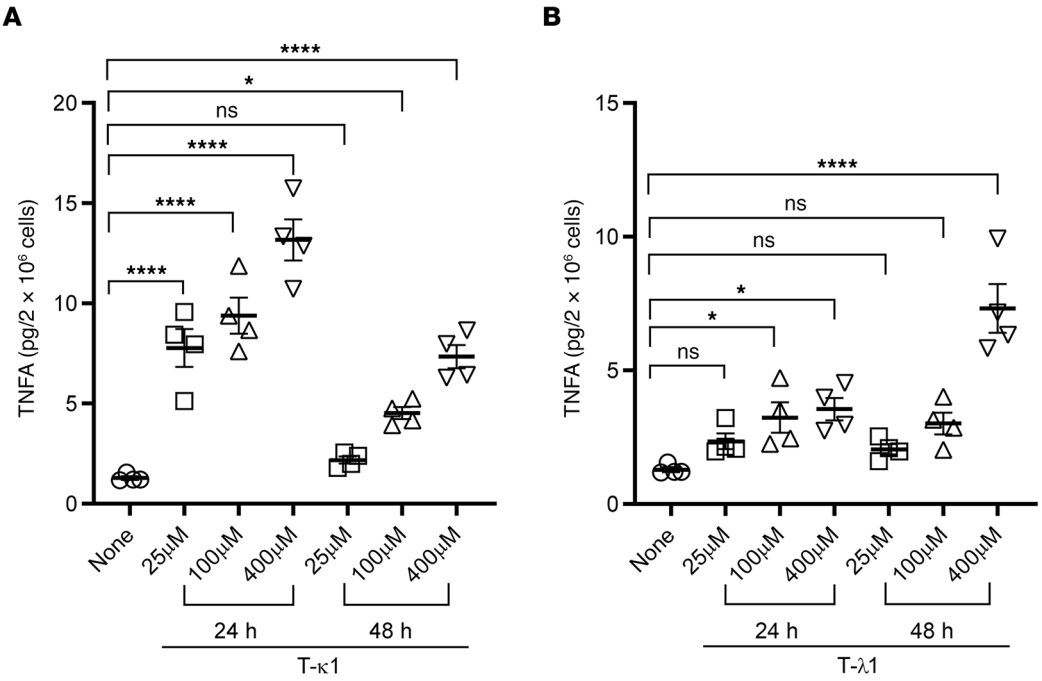

Figure 3. TNFA levels increased in PTCs in a dose- and time-dependent manner after exposure to either FLC isotype. PTCs (RPTECs) incubated with FLCs (**A**) T-κ1 and (**B**) T-λ1 increased secretion of TNF-α ($P < 0.05$; $n = 4$) in a dose- and time-dependent manner. *$P < 0.05$, ****$P < 0.0001$ (1-way ANOVA followed by Tukey's multiple comparisons test). PTCs, proximal tubule cells; FLCs, free light chains.

TLRs are currently being explored as therapy targets because interference with their signaling pathways can limit tumor formation. Enhancing their activity could provide an adjuvant therapy to standard treatments (28). Our current knowledge of the function of TLRs has gone beyond the main role as triggers of innate and adaptive immune responses (29–31). TLRs play a major role in the pathogenesis of hypoxia/ischemia-induced acute kidney injury (AKI) and other types of AKI (32–35). In the present study, we have aimed to explore the pathophysiologic role of TLRs in FLC-induced injury in kidney PTCs. Our data showed that TLRs may be major mediators of human FLC-induced PTC injury.

The present studies also demonstrated that FLCs promoted a STAT1-dependent release of HMGB1. High mobility group (HMG) proteins comprise a large superfamily that has 3 subfamilies: HMGA, HMGB, and HMGN. HMGs have a common carboxyl terminus, but each has a unique functional motif that confers distinct cellular functions (36). These nuclear proteins are involved in the regulation of chromatin dynamics. However, HMGB1 in particular is released into the extracellular fluid in inflammatory states (37). Unlike the other 2 HMGB family members, HMGB1 promotes additional biological functions by serving as a ligand particularly for TLR2 and TLR4 to effect the elaboration of cytokines and chemokines (38). As a prototypical alarmin, which is an endogenously derived danger signal molecule (37), HMGB1 was produced by PTCs exposed to FLCs and directly involved in the inflammatory responses mediated through the TLRs.

Proximal tubulopathy and "myeloma kidney," which is now known as cast nephropathy, comprise the 2 most common types of kidney involvement in patients with MM. Proximal tubulopathy may be associated with tubule dysfunction including proximal tubular acidosis (type 2) clinically. Cast nephropathy is predominantly a chronic tubulointerstitial disease that spares the glomeruli and is characterized by interstitial fibrosis and tubule atrophy as well as tubule casts formed by binding of FLCs to Tamm-Horsfall protein (1, 7, 8, 39). FLCs are responsible for the majority of kidney lesions seen in myeloma. The occurrence of casts in myeloma kidney is highly variable: it may be extensive in some cases, especially in acute cast nephropathy, and exceedingly sparse in others. In either case, there is a prominent feature of tubulointerstitial injury with extensive fibrosis and tubule atrophy. The present study elaborates a mechanism whereby some FLCs facilitate fibrosis and tubule atrophy by

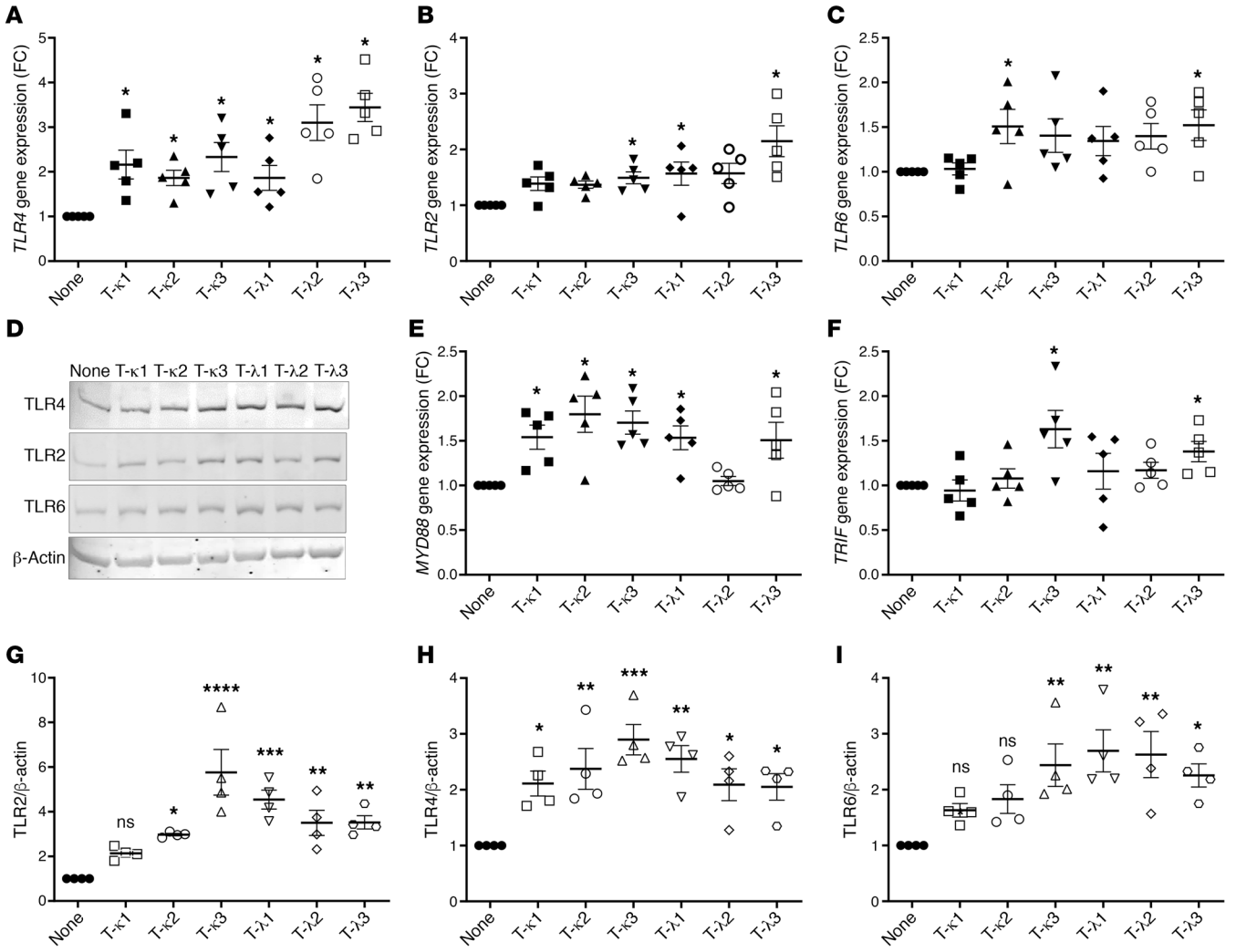

Figure 4. FLCs upregulated the expression of TLR2, TLR4, and TLR6 as well as their downstream adaptor protein molecules, MYD88 and TRIF. (**A–D** and **G–I**) FLCs significantly upregulated gene/protein expression of TLR2, TLR4, and TLR6 and their adaptor protein molecules (**E**) MYD88 and (**F**) TRIF (*P < 0.05; n = 5) in PTCs (RPTECs). *P < 0.05, **P < 0.01, ***P < 0.001, ****P < 0.0001 (1-way ANOVA followed by Tukey's multiple comparisons test). FLCs, free light chains; PTCs, proximal tubule cells.

causing cell injury in the absence of obstructive casts. These studies confirm the pivotal role of STAT1 in initiating these inflammatory responses through the release of HMGB1, a major ligand responsible for the activation of TLRs, from injured PTCs. The findings further suggest pathways for intervention in limiting chronic kidney disease in MM.

Methods

Subject population. Twelve different FLCs, 6 κ and 6 λ, were isolated and purified from patients with MM from Tulane Hospital, Memorial Sloan Kettering Cancer Center, and the University of Alabama at Birmingham. All 12 patients had mild to moderate kidney disease with light chain proteinuria but without significant albuminuria, comprising a group of patients predominantly with tubulointerstitial disease.

Urine collection and FLC isolation. FLCs were purified from the urine of patients who had multiple myeloma, light chain proteinuria, and clinical evidence of significant renal damage that was presumed to be cast nephropathy, using standard methods described previously (3, 12, 22, 24). Briefly, urine samples were precipitated with ammonium sulfate (Millipore Sigma, catalog A-5132) (55% to 90% saturation, determined empirically), extensively dialyzed against distilled water and lyophilized. To purify the crude FLCs, they were dissolved in buffer at pH 6.0 followed by chromatography on CM-Sephadex C-50 (Millipore Sigma, catalog C-50120) column; bound FLCs were eluted with 0.6 M of NaCl, redialyzed

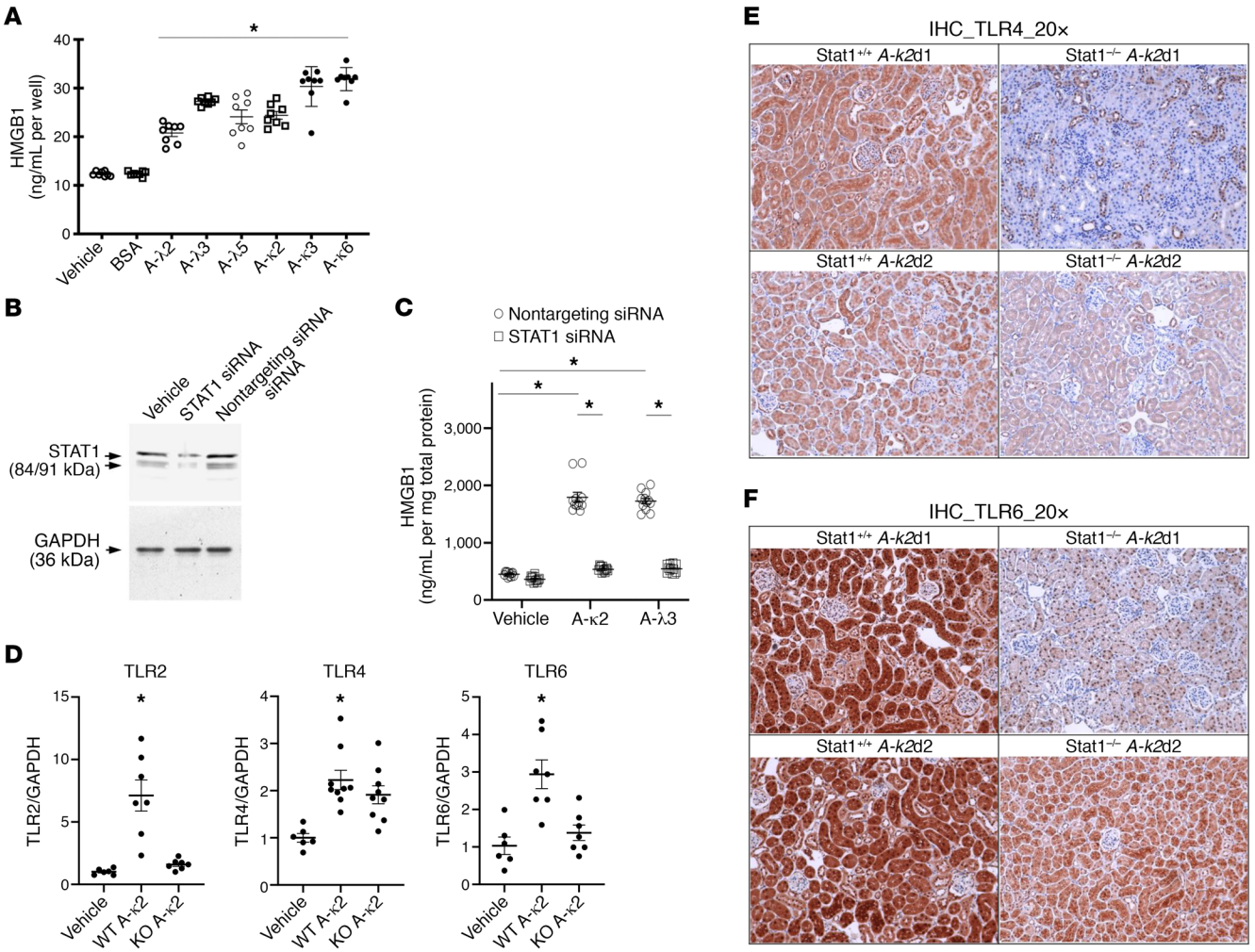

Figure 5. FLCs induced HMGB1 release and TLR2/TLR 4/TLR6 expression in vivo, which was mitigated in *STAT1*$^{-/-}$ mice. (**A**) Six different FLCs (n = 8 samples in each group) increased the release of HMGB1 compared with vehicle-treated cells and cells incubated in medium containing BSA, 5 mg/ml (*P < 0.0001). Data were analyzed using 1-way ANOVA. (**B**) Treatment with siRNA reduced STAT1 protein levels by about 70%–75%; no effect of the nontargeting siRNA on STAT1 was observed. (**C**) Knockdown of STAT1 inhibited FLC-induced increases in HMGB1 (n = 12 samples in each group) by HK-2 cells. Concentration of HMGB1 in medium was divided by total protein of cellular lysates in each sample. Data were analyzed using 2-way ANOVA. The analysis comparing the main effects of the FLC and the interaction effect between the FLC and siRNA on HMGB1 showed the main effect for FLC yielded an F ratio of F(2, 66) = 228.1, P < 0.0001, and the effect of siRNA yielded an F ratio of F(1, 66) = 654.3, P < 0.0001. The interaction effect was significant: F ratio of F(2, 66) = 133.2, P < 0.0001. *P < 0.0001. (**D**) FLCs induced TLR2, TLR4, and TLR6 gene expression significantly in WT mice but not in *Stat1*$^{-/-}$ mice. (**E** and **F**) Representative IHC slides from WT and *Stat1*$^{-/-}$ mice. The WT mice treated with FLCs showed positive staining for TLR4 (**E**, left) and TLR6 (**F**, left); *Stat1*$^{-/-}$ kidneys were negative or weakly positive (**E** and **F**, left). A-κ2- d1 and d2 denote different doses of FLCs injected to mice. Lower dose (termed κ2-d1 = 0.033 mg/g BW) or higher dose (termed κ2-d2 = 0.165 mg/g BW) of κ2 FLC in PBS. Untreated controls were negative. FLCs, free light chains.

and lyophilized. The purity and identity of FLCs were confirmed by SDS-PAGE and Western blotting. FLCs, isolated from the urine and purified and stored in lyophilized form, were used for the experiments. The FLCs from the UAB laboratory were labeled A-κ2, A-κ3, A-κ6, A-λ2, A-λ3, and A-λ5. The FLCs from Tulane were labeled as T-κ1, T-κ2, T-κ3, T-λ1, T-λ2, and T-λ3. All specimens were determined to be endotoxin-free. FLCs were pathogen- and endotoxin-free.

Cell cultures. We used human kidney PTCs (cell lines: RPTECs [ATCC, catalog CRL-4031] and HK2 [ATCC, catalog CRL-2190] to evaluate the effect of κ and λ light chains. We cultured and prepared cells for experiments as previously described (4, 11, 22, 24, 40). Briefly, cells were grown (passage <10) on CellBIND surface flasks/6-well plates (Corning) and incubated at 37°C with 5% CO2. RPTECs were cultured in DMEM/F12 medium (ATCC, catalog 30-2006) with REGM SingleQuots Supplements Kit and growth factors (Lonza, catalog CC-4127), and HK2 cells were cultured in keratinocyte serum-free medium (catalog 10744019) (Gibco, Invitrogen, Thermo Fisher Scientific) supplemented with recombinant human epidermal

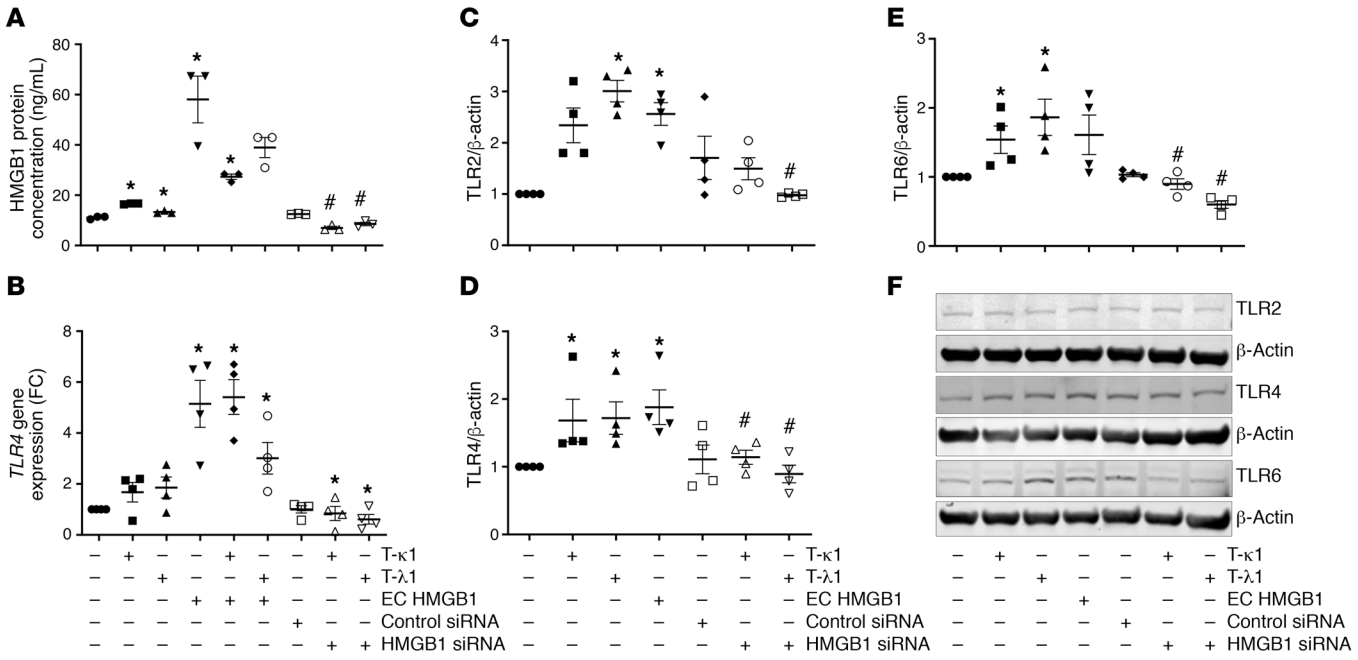

Figure 6. FLCs activated TLRs through HMGB1, and HMGB1 acts as a regulator of TLR2, TLR4, and TLR6 activation in PTCs. (**A**) Release of HMGB1 into the medium from cells (RPTECs) exposed to the FLCs and HMGB1 modulators. (**B–F**) Effect of HMGB1 modulation on the expression of TLR2, TLR4, and TLR6 proteins; extracellular HMGB1 used as HMGB1 mimic and HMGB1 siRNA was used as an inhibitor. $^{\#}P < 0.05$, compared with FLCs; $^{*}P < 0.05$, compared with no LC (k or λ) (1-way ANOVA followed by Tukey's multiple comparisons test). FLCs, free light chains.

growth factor (5 ng/mL) and bovine pituitary extract (50 μg/mL). Media was exchanged at 48-hour intervals. The cells were exposed to both κ and λ FLCs at varying doses and time intervals. Cell supernatant was collected for ELISA and cell pellet was used for gene expression studies. Based on our dose-time screening data, we used a minimum concentration of FLCs (25 μM) for a minimum exposure time of 24 hours.

Animal and tissue preparation. Colonies of *Stat1* knockout mice (termed *Stat1*$^{-/-}$ mice) and littermate controls (termed *Stat*$^{+/+}$ mice) were developed and confirmed by PCR-based genotyping and maintained in a gnotobiotic facility, as described previously (5). All animal studies were conducted using animal biosafety level–3 laboratory and Sealsafe cages with HEPA filters, and personnel wore personal protective equipment. *Stat1*$^{-/-}$ mice grew normally and were phenotypically normal under these conditions. Eight-week-old male *Stat1*$^{+/+}$ and *Stat1*$^{-/-}$ mice (n = 8–10/group) were i.p. injected daily with either PBS alone (Invitrogen) as vehicle or with the κ2 FLC at a lower dose (termed κ2-d1 = 0.033 mg/g BW or higher dose (termed κ2-d2 = 0.165 mg/g BW) of κ2 FLC in PBS. The experiments were concluded on day 10 and the left kidney was harvested for histology and IHC (5).

Cell proliferation assay. To check the effect of FLCs on proliferation of PTCs, CellTiter 96 AQueous One Solution Cell Proliferation Assay (MTS) (Promega, catalog G3580) was used. Cells were seeded in 96-well plates (1.0×10^4 cells/well) and exposed to FLCs for indicated time periods followed by the MTS assay. MTS assays were performed by adding a small amount (20 μL) of the CellTiter 96 AQueous One Solution Reagent directly to the culture wells, incubating for 2 hours, and then recording absorbance at 490 nm with BioTek Synergy HT Multi-Detection Microplate Reader (BioTek).

Immunocytochemistry. Immunofluorescence microscopy was performed using 4% paraformaldehyde-fixed HK2 cells. Cells were permeabilized with Triton X-100 (0.1%) and BSA (2%) in PBS. Cells were blocked in normal goat serum (Cell Signaling Technology, catalog 5425S) plus 0.1% Triton X-100 (PBST) for 1 hour. Slides were incubated in LCN2 primary antibody (dilution 1:100; Abcam, catalog Ab63929) that were diluted in blocking buffer overnight at 4°C. Cells were washed in PBST (3 times). Goat anti–rabbit IgG (H+L) Superclonal Secondary Antibody, Alexa Fluor 555 (Thermo Fisher Scientific, catalog A27039) was used at a concentration of 1.0 μg/mL (1:1000) in PBS containing 0.2% BSA for 1 hour at room temperature. Samples were then washed in PBST and rinsed in phosphate buffer; no. 1.5 coverslips

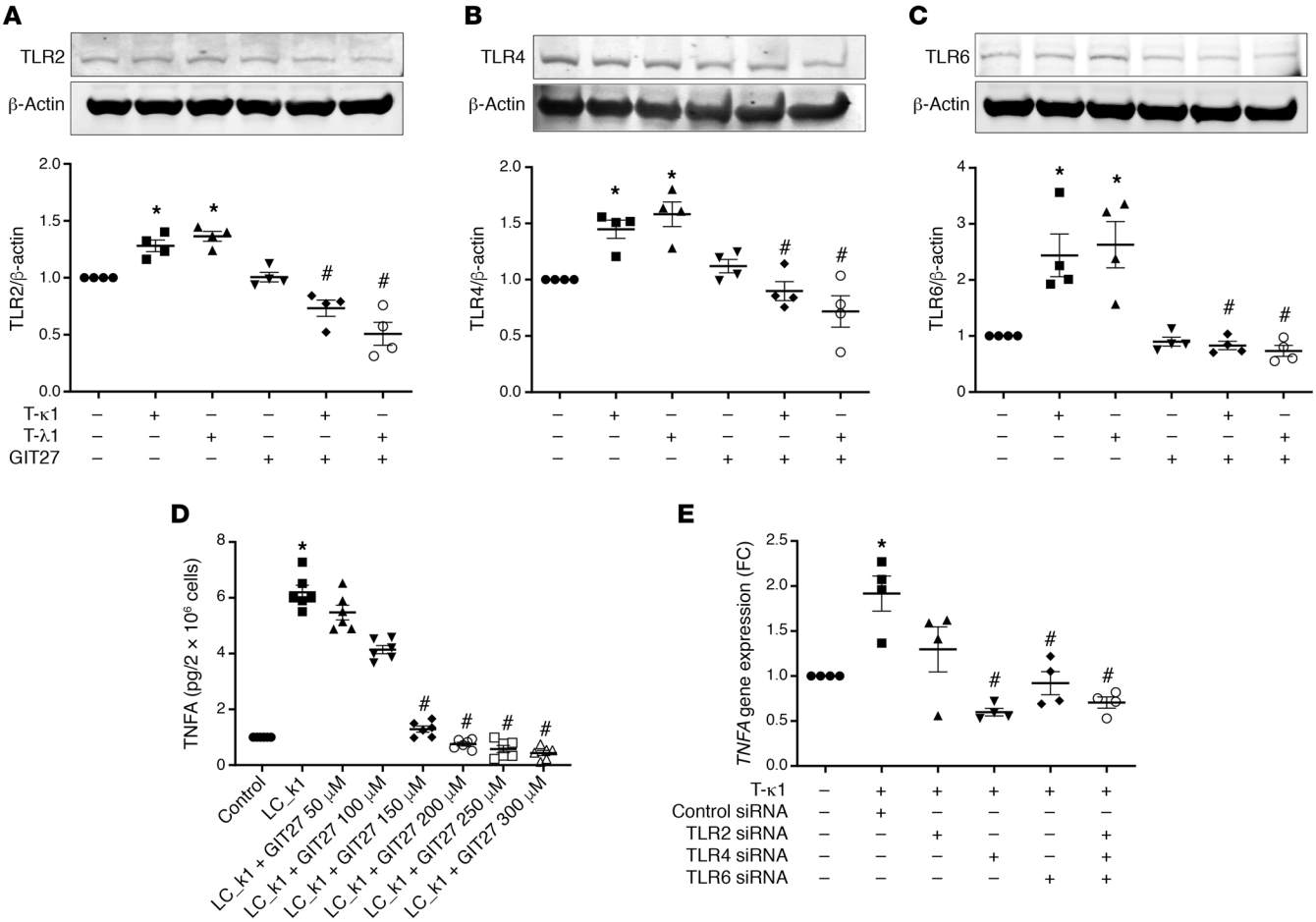

Figure 7. Inhibition of TLR expression reduced FLC-induced TNF-α release by PTCs. (**A–D**) Effect of TLR inhibitor 4,5-dihydro-3-phenyl-5-isoxazoleacetic acid (GIT27) and (**E**) pooled TLR2/4/6-siRNA on TNF-α release by PTCs (RPTECs). $n = 4$; $^{\#}P < 0.05$, compared with FLCs; $^{*}P < 0.05$, compared with no LC (k or λ) (1-way ANOVA followed by Tukey's multiple comparisons test). PTCs, proximal tubule cells.

were mounted with UltraCruz Aqueous Mounting Medium with DAPI (Santa Cruz Biotechnology, catalog sc-24941). Images were captured on an upright Nikon Eclips 80i fluorescent microscope (NIKON) (original magnification ×40).

Molecular inhibitors/mimics and siRNA transfections. To knock down the expression of a specific gene, we used commercially available siRNAs or known molecular inhibitors. *Stat1* siRNA (OriGene Technology, catalog SR304620), HMGB1 siRNA (Ambion, Thermo Fisher Scientific, catalog AM16708), pooled siRNA (3 to 5 target-specific) for TLR2 (Santa Cruz Biotechnology, catalog sc-40256), TLR4 (Santa Cruz Biotechnology, catalog sc-40260), TLR6 (Santa Cruz Biotechnology, catalog sc-40264), megalin siRNA (Santa Cruz Biotechnology, catalog sc-40103), and cubilin siRNA (Santa Cruz Biotechnology, catalog sc-40100) were used for corresponding gene knockdown experiments. As a control for transfection, control siRNA-A (Santa Cruz Biotechnology, catalog sc-37007) was used, which consists of a scrambled sequence.

Molecular inhibitors used to inhibit HMGB1 were R,S Sulforaphane (3 μM, Enzo Life Sciences, catalog ALX-350-232-M025), TLR2,4,6 (GIT27, 150 μM, TOCRIS, Bio-Techne, catalog 3270), and endocytosis inhibitor (bafilomycin, 1 μM, MilliporeSigma, catalog B1793). As a molecular mimic, extracellular HMGB1 (100 ng/mL, MilliporeSigma, catalog SRP6265) was used to modulate HMGB1 expression in cultured RPTECs in presence or absence of FLCs.

ELISA. The levels of TNF-α and HMGB1 in the cell culture medium were determined with ELISA kits (Thermo Fisher Scientific, catalog BMS223-4, and Tecan, catalog ST51011, respectively) according to the manufacturer's instructions.

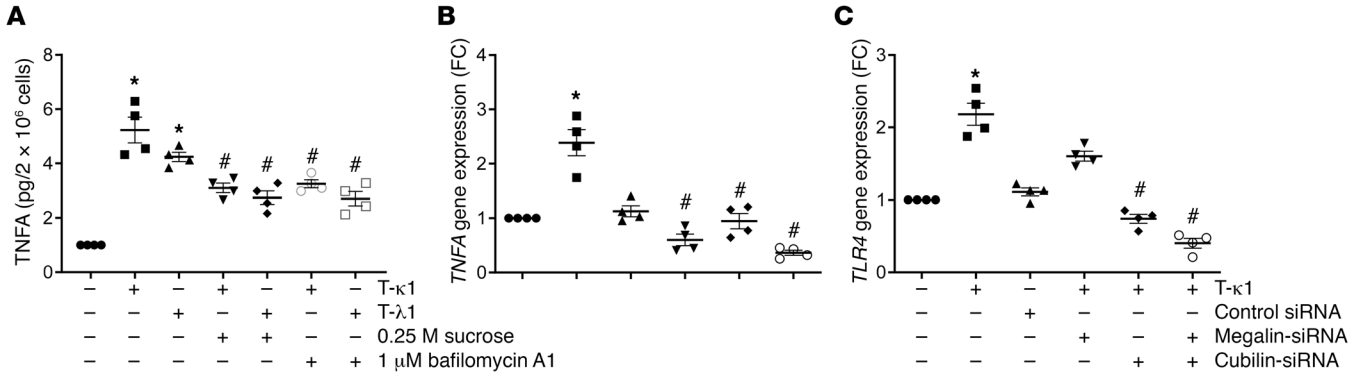

Figure 8. Blocking endocytosis of FLCs inhibited TNFA release and expression of TLR4 and TNFA. Blocking endocytosis with hypertonic sucrose (0.25 M), (**A** and **B**) bafilomycin A1 (1 μM) or cubilin/megalin siRNA ameliorated FLC-induced TNF-α release in PTCs (RPTECs). (**C**) Cubilin/megalin siRNA synergistically lowered the FLC-induced TLR4 expression in PTCs (RPTECs). $n = 4$; $^{\#}P < 0.05$, compared with FLCs; $^{*}P < 0.05$, compared with no LC (k or λ) (1-way ANOVA followed by Tukey's multiple comparisons test). FLCs, free light chains; PTCs, proximal tubule cells.

Real-time qPCR (RT-qPCR). Total RNA was isolated from cultured PTCs using the RNeasy Plus Mini Kit (QIAGEN, catalog 74136). Total RNA (0.2–1 μg) of purified RNA was used to prepare cDNA through high-capacity RNA to c-DNA kit (Applied Biosystems, catalog 4368814). Candidate gene expressions were estimated using the fluorescent dye SYBR Green methodology and CFX96 Touch Real-Time PCR machine (Bio-Rad). Bioinformatically validated primer sets (QuantiTect Primer Assays, QIAGEN, or IDT) were purchased for use in SYBR Green-based RT-PCR. Real-time fluorescence from SYBR Green (Applied Biosystems) was measured by the Bio-Rad CFX Manager 3.1 System Software. Gene expression was normalized to the endogenous controls (β-actin or *GAPDH*) and comparative CT values were estimated. Relative gene expression was calculated through $2^{-(\Delta\Delta CT)}$ method and expressed in arbitrary units (a.u.) relative to paired controls. Heatmap of gene expressions was generated by using the "Heatmapper" web server (41). Hierarchical clustering was done as Average Linkage and Euclidian method was used for distance measurement between clusters.

To analyze the expression of TLRs in mice, total RNA was extracted from kidney cortex with TRIzol (Invitrogen, catalog 15596018), treated with DNAase I (Invitrogen, catalog 18068015) to remove carry over genomic DNA, and then purified with use of an RNA purification kit (Ambion). The DNA-free RNA was reverse-transcribed to cDNA with SuperScript IV (Invitrogen, catalog 18090200). Candidate gene expressions were estimated using the fluorescent dye SYBR Green methodology and Roche LightCycler480 Real-Time PCR machine (Roche). Primer sets (IDT) were purchased for use in SYBR Green-based RT-PCR. Real-time fluorescence from SYBR Green (Applied Biosystems) was measured by the LightCycler480 System Software. Gene expression was normalized to the endogenous controls GAPDH and comparative CT values were estimated. Relative gene expression was calculated through $2^{-(\Delta\Delta CT)}$ method and expressed in fold-change relative to the vehicle control group.

Western blotting. Protein was isolated from cells and quantified through Pierce BCA Protein Assay Kit (Thermo Fisher Scientific, catalog 23225). Immunoblotting was done to detect the expression of proteins with antibodies against TLR2 (dilution 1:200; Santa Cruz Biotechnology, catalog sc-21759), TLR4 (dilution 1:200; Santa Cruz Biotechnology, catalog sc-293072), TLR6 (dilution 1:1000; ProSci, catalog 3651), and β-actin (dilution 1:1000; LI-COR Biotechnology, catalog 926-42212). Equal amounts of proteins (10–20 μg) were separated through Bolt 4%–12% Bis-Tris Gel (Thermo Fisher Scientific, catalog NW04122BOX) electrophoresis and transferred onto nitrocellulose membrane (LI-COR Biotechnology, catalog 926-31092). The membrane was blocked with PBS, TBS, or 5% milk in Tris-Buffered Saline-Tween (0.05%) solution based on primary antibody–specific recommendations of the manufacturer. After overnight incubation with primary antibody, blots were incubated with LI-COR secondary antibody (Odyssey IRDye 680RD, catalog 926-68070 or 800CW, catalog 926-32211) for 1 hour. Western blots were visualized by Odyssey CLx Imaging System (LI-COR Biotechnology) using near-infrared fluorescence capture. Western blot image analysis was done using Image Studio software (LI-COR Biotechnology) to obtain the integrated intensities. Data analysis was done after normalizing with endogenous control protein (β-actin or GAPDH).

IHC for TLRs. IHC for TLR2, TLR4, and TLR6 was performed in kidney sections prepared from the same *Stat1*$^{+/+}$ and *Stat1*$^{-/-}$ mice studied by Ying et al. in recently reported experiments, which demonstrated that the STAT1 served as the key signaling molecule that produced the proinflammatory molecule IL-1ß as well as the profibrotic agent TGF-β in the proximal tubule epithelium (5). Immunostaining was done following a standard protocol at Tulane pathology core facility. Briefly, slides were dispensed in 150 μL reagents in each step. Blocking was performed with 5 minutes incubation in H_2O_2, 10 minutes each with Avidin and Biotin (Biocare Medical, catalog AB972L) for auxiliary blocking. Retrieval step was performed manually at pH 6.0 with citrate rodent solution (Biocare Medical, catalog CB910M) and NxGen Decloaker (Biocare Medical, catalog RD9132) was used for 15 minutes at 110°C. After rinsing, nonspecific proteins were blocked for 30 minutes with Rodent Block M (Biocare Medical, catalog RBM961 G). Slides were rinsed and incubated for 45 minutes with TLR4 (dilution 1:250, Santa Cruz Biotechnology, catalog sc-293072) and TLR6 (dilution 1:100, ProSci, catalog 3651) primary antibodies. Da Vinci Green (Biocare Medical, catalog PD900 H) diluent was used for antibody dilutions. Slides were incubated with secondary antibodies for 30 minutes; mouse-on-mouse HRP (Biocare Medical, catalog MM620) and rabbit-on-rodent (Biocare Medical, catalog RMR 622) secondary antibodies were used for TLR4 and TLR6 staining, respectively. DAB was incubated for 5 minutes as substrate and CAT-Hematoxylin (Biocare Medical, catalog CATHE-M) was used in 1:5 dilution in 1x TBS buffer for counterstaining. Biocare Nemesis (LVMA-LV1.3-0187) automated stainer was used to run all experimental slides under uniform conditions. Stained sections were imaged at original magnification, ×20, using fluorescent microscope (M5000, Thermo Scientific) and representative images were used for scorings.

The staining intensity of the TLR4 and TLR6 as well as the 1:5 CAT Hematoxylin counterstaining as a labeling index (percentage of positive nuclei) was evaluated and scored by a single, experienced pathologist. The paraffin sections were prepared from *Stat1*$^{+/+}$ and *Stat1*$^{-/-}$ mice previously reported by Ying et al. (5), and the sections were coded such that the pathologist was blinded to the experimental design and the source of the kidney sections. TLR2 staining yielded no staining in the *Stat1*$^{+/+}$ or *Stat1*$^{-/-}$ mice. TLR4 and TLR6 staining were interpretable and the slides were scored as 0 (absence of staining) (negative), 1+ (weakly positive), 2 + (moderately positive), and 3+ (intense staining) (strongly positive).

Statistics. Data were analyzed by comparing mean values through either 2-tailed Student's *t* test or 1-way ANOVA (for comparing multiple groups) or 2-way ANOVA with Tukey's multiple comparison post hoc test. *P* values of less than 0.05 were assumed significant. Data were expressed as mean ± SEM. Data were analyzed by using GraphPad Prism software, version 8.3.0. All experiments were performed at least in triplicate.

Study approval. This study was approved by the IRB at the Tulane Office of Human Research Protection (IRB reference no. 848169), and all protected health information was deidentified. In addition, the Birmingham VA IRB provided annual continuing IRB oversight and approval of this research activity. This study was carried out in strict accordance with the recommendations in the *Guide for the Care and Use of Laboratory Animals* (National Academies Press, 2011). The Institutional Animal Care and Use Committee at the University of Alabama at Birmingham approved the project.

Author contributions

VB and RU conceived the study and designed experiments. VB and PWS secured funding for the project and helped with manuscript preparation. RU, ZN, WZY, and WF designed and performed the experiments and analyzed data. RU, VB, and PWS wrote and edited the manuscript. HS enrolled MM patients for the study. EAJ contributed in the study design and provided inputs in drafting manuscript All authors read the manuscript, provided input and approved the final submission. PWS and VB contributed equally to this work.

Acknowledgments

This work was supported by Paul Teschan Research Fund (to VB), by a Merit Award (1 I01 CX001326) from the United States Department of Veterans Affairs Clinical Sciences R&D (CSRD) Service (to PWS) and a NIH George M. O'Brien Kidney and Urological Research Centers Program (P30 DK079337) (to PWS), and by P30CA008748 (to EAJ).

Address correspondence to: Vecihi Batuman, Division of Nephrology and Hypertension, John W. Deming Department of Medicine, Tulane University School of Medicine, SL-45, 1430 Tulane Avenue, New Orleans, Louisiana 70112, USA. Phone: 504.988.5346; Email: vbatuma@tulane.edu.

1. Hutchison CA, et al. The pathogenesis and diagnosis of acute kidney injury in multiple myeloma. *Nat Rev Nephrol*. 2011;8(1):43–51.
2. Batuman V. Proximal tubular injury in myeloma. *Contrib Nephrol*. 2007;153:87–104.
3. Batuman V, et al. Myeloma light chains are ligands for cubilin (gp280). *Am J Physiol*. 1998;275(2):F246–F254.
4. Li M, Balamuthusamy S, Simon EE, Batuman V. Silencing megalin and cubilin genes inhibits myeloma light chain endocytosis and ameliorates toxicity in human renal proximal tubule epithelial cells. *Am J Physiol Renal Physiol*. 2008;295(1):F82–F90.
5. Ying WZ, Li X, Rangarajan S, Feng W, Curtis LM, Sanders PW. Immunoglobulin light chains generate proinflammatory and profibrotic kidney injury. *J Clin Invest*. 2019;129(7):2792–2806.
6. Sirac C, et al. Animal models of monoclonal immunoglobulin-related renal diseases. *Nat Rev Nephrol*. 2018;14(4):246–264.
7. Doshi M, Lahoti A, Danesh FR, Batuman V, Sanders PW, American Society of Nephrology Onco-Nephrology Forum. Paraprotein-related kidney disease: kidney injury from paraproteins-what determines the site of injury? *Clin J Am Soc Nephrol*. 2016;11(12):2288–2294.
8. Sanders PW. Mechanisms of light chain injury along the tubular nephron. *J Am Soc Nephrol*. 2012;23(11):1777–1781.
9. Batuman V. The pathogenesis of acute kidney impairment in patients with multiple myeloma. *Adv Chronic Kidney Dis*. 2012;19(5):282–286.
10. Khan AM, Li M, Balamuthusamy S, Maderdrut JL, Simon EE, Batuman V. Myeloma light chain-induced renal injury in mice. *Nephron Exp Nephrol*. 2010;116(2):e32–e41.
11. Li M, Hering-Smith KS, Simon EE, Batuman V. Myeloma light chains induce epithelial-mesenchymal transition in human renal proximal tubule epithelial cells. *Nephrol Dial Transplant*. 2008;23(3):860–870.
12. Batuman V, Guan S. Receptor-mediated endocytosis of immunoglobulin light chains by renal proximal tubule cells. *Am J Physiol*. 1997;272(4 Pt 2):F521–F530.
13. Sanders PW. Light chain-mediated tubulopathies. *Contrib Nephrol*. 2011;169:262–269.
14. Ying WZ, Sanders PW. Mapping the binding domain of immunoglobulin light chains for Tamm-Horsfall protein. *Am J Pathol*. 2001;158(5):1859–1866.
15. Lu B, et al. JAK/STAT1 signaling promotes HMGB1 hyperacetylation and nuclear translocation. *Proc Natl Acad Sci U S A*. 2014;111(8):3068–3073.
16. Knudsen LM, Hippe E, Hjorth M, Holmberg E, Westin J. Renal function in newly diagnosed multiple myeloma — a demographic study of 1353 patients. The Nordic Myeloma Study Group. *Eur J Haematol*. 1994;53(4):207–212.
17. Nasr SH, et al. Clinicopathologic correlations in multiple myeloma: a case series of 190 patients with kidney biopsies. *Am J Kidney Dis*. 2012;59(6):786–794.
18. Masai R, et al. Clinicopathological features and prognosis in immunoglobulin light and heavy chain deposition disease. *Clin Nephrol*. 2009;71(1):9–20.
19. Gertz MA. Managing light chain deposition disease. *Leuk Lymphoma*. 2012;53(2):183–184.
20. Mohan M, et al. Clinical characteristics and prognostic factors in multiple myeloma patients with light chain deposition disease. *Am J Hematol*. 2017;92(8):739–745.
21. Cancer Stat Facts: Myeloma. Cancer Stat Facts: Myeloma. National Cancer Institute: National Cancer Institute. https://seer.cancer.gov/statfacts/html/mulmy.html. Accessed July 13, 2020.
22. Sengul S, Zwizinski C, Simon EE, Kapasi A, Singhal PC, Batuman V. Endocytosis of light chains induces cytokines through activation of NF-κB in human proximal tubule cells. *Kidney Int*. 2002;62(6):1977–1988.
23. Li M, Maderdrut JL, Lertora JJ, Arimura A, Batuman V. Renoprotection by pituitary adenylate cyclase-activating polypeptide in multiple myeloma and other kidney diseases. *Regul Pept*. 2008;145(1–3):24–32.
24. Sengul S, Erturk S, Khan AM, Batuman V. Receptor-associated protein blocks internalization and cytotoxicity of myeloma light chain in cultured human proximal tubular cells. *PLoS One*. 2013;8(7):e70276.
25. Sengul S, Li M, Batuman V. Myeloma kidney: toward its prevention — with new insights from in vitro and in vivo models of renal injury. *J Nephrol*. 2009;22(1):17–28.
26. Arimura A, Li M, Batuman V. Treatment of renal failure associated with multiple myeloma and other diseases by PACAP-38. *Ann N Y Acad Sci*. 2006;1070:1–4.
27. El-Achkar TM, Dagher PC. Renal Toll-like receptors: recent advances and implications for disease. *Nat Clin Pract Nephrol*. 2006;2(10):568–581.
28. Thakur KK, et al. Role of toll-like receptors in multiple myeloma and recent advances. *Exp Hematol*. 2015;43(3):158–167.
29. Abdi J, Garssen J, Redegeld F. Toll-like receptors in human multiple myeloma: new insight into inflammation-related pathogenesis. *Curr Mol Med*. 2014;14(4):423–431.
30. Abdi J, Mutis T, Garssen J, Redegeld F. Characterization of the Toll-like receptor expression profile in human multiple myeloma cells. *PLoS One*. 2013;8(4):e60671.
31. Abdi J, Mutis T, Garssen J, Redegeld FA. Toll-like receptor (TLR)-1/2 triggering of multiple myeloma cells modulates their adhesion to bone marrow stromal cells and enhances bortezomib-induced apoptosis. *PLoS One*. 2014;9(5):e96608.
32. Amura CR, Renner B, Lyubchenko T, Faubel S, Simonian PL, Thurman JM. Complement activation and toll-like receptor-2 signaling contribute to cytokine production after renal ischemia/reperfusion. *Mol Immunol*. 2012;52(3-4):249–257.
33. Arumugam TV, Okun E, Tang SC, Thundyil J, Taylor SM, Woodruff TM. Toll-like receptors in ischemia-reperfusion injury. *Shock*. 2009;32(1):4–16.
34. Khan AM, Li M, Abdulnour-Nakhoul S, Maderdrut JL, Simon EE, Batuman V. Delayed administration of pituitary adenylate

cyclase-activating polypeptide 38 ameliorates renal ischemia/reperfusion injury in mice by modulating Toll-like receptors. *Peptides*. 2012;38(2):395–403.
35. Li M, Khan AM, Maderdrut JL, Simon EE, Batuman V. The effect of PACAP38 on MyD88-mediated signal transduction in ischemia-/hypoxia-induced acute kidney injury. *Am J Nephrol*. 2010;32(6):522–532.
36. Hock R, Furusawa T, Ueda T, Bustin M. HMG chromosomal proteins in development and disease. *Trends Cell Biol*. 2007;17(2):72–79.
37. Diener KR, Al-Dasooqi N, Lousberg EL, Hayball JD. The multifunctional alarmin HMGB1 with roles in the pathophysiology of sepsis and cancer. *Immunol Cell Biol*. 2013;91(7):443–450.
38. Bianchi ME, Manfredi AA. High-mobility group box 1 (HMGB1) protein at the crossroads between innate and adaptive immunity. *Immunol Rev*. 2007;220:35–46.
39. Ying WZ, Allen CE, Curtis LM, Aaron KJ, Sanders PW. Mechanism and prevention of acute kidney injury from cast nephropathy in a rodent model. *J Clin Invest*. 2012;122(5):1777–1785.
40. Sengul S, Zwizinski C, Batuman V. Role of MAPK pathways in light chain-induced cytokine production in human proximal tubule cells. *Am J Physiol Renal Physiol*. 2003;284(6):F1245–F1254.
41. Babicki S, et al. Heatmapper: web-enabled heat mapping for all. *Nucleic Acids Res*. 2016;44(W1):W147–W153.